Hyperfine Interact (2016) 237: 6
DOI 10.1007/s10751-016-1220-x

Iron oxide and iron carbide particles produced by the polyol method

Y. Yamada[1] · R. Shimizu[1] · Y. Kobayashi[2,3]

Published online: 18 February 2016

Abstract Iron oxide (γ-Fe_2O_3) and iron carbide (Fe_3C) particles were produced by the polyol method. Ferrocene, which was employed as an iron source, was decomposed in a mixture of 1,2-hexadecandiol, oleylamine, and 1-octadecene. Particles were characterized using Mössbauer spectroscopy, X-ray diffraction, and transmission electron microscopy. It was found that oleylamine acted as a capping reagent, leading to uniform-sized (12-16 nm) particles consisting of γ-Fe_2O_3. On the other hand, 1-octadecene acted as a non-coordinating solvent and a carbon source, which led to particles consisting of Fe_3C and α-Fe with various sizes.

Keywords Nanoparticles · Polyol method · Iron oxide · Iron carbide · Mössbauer spectroscopy

1 Introduction

Iron-based particles have attracted considerable attention because of their applicability to magnetic materials and catalysis. Iron carbide (Fe_3C) nanoparticles show a higher saturation magnetization than Fe_3O_4 [1]. In terms of basic science, the study of particles yields important information on metastable lattice structures unobtainable in bulk solids, as the surface

This article is part of the Topical Collection on *Proceedings of the International Conference on the Applications of the Mössbauer Effect (ICAME 2015), Hamburg, Germany, 13-18 September 2015*

✉ Y. Yamada
yyasu@rs.kagu.tus.ac.jp

[1] Department of Chemistry, Tokyo University of Science, Kagurazaka, Shinjuku, Tokyo, Japan

[2] Graduate School of Informatics and Engineering, The University of Electro-Communications, Chofugaoka, Chofu, Tokyo, Japan

[3] Nishina Center for Accelerator-Based Science, RIKEN, Hirosawa, Wako, Saitama, Japan

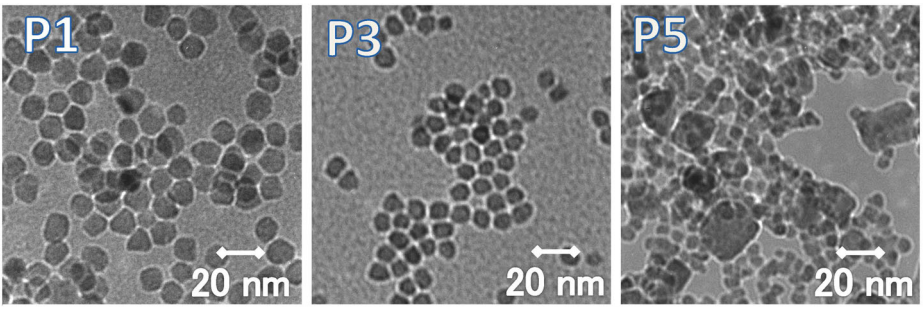

Fig. 1 TEM images of selected P1, P3, and P5 particles

energy is enhanced in nano-sized particles. Various methods to produce iron-based particles have been reported, such as ball milling, laser ablation, and sonochemical methods. Among these methods, the polyol method is conducive to producing metallic particles having a uniform size. Polyol acts as a reducing agent. It simultaneously prevents particle aggregation, which controls growth. In previous studies, $Fe(acac)_3$ [2] or $Fe(CO)_5$ [3] was used as an iron source to produce iron oxide particles. We have previously reported novel iron sulfide (Fe_2S_3) particles produced by the polyol method, where ferrocene was employed as an iron source and 1-octadecanthiol was added into the solution as a sulfur source [4, 5]. Generally, it is hard to obtain Fe metal particles by reducing Fe cations using polyol, though some studies have successively produced Fe^0 compounds: FePt alloy particles [6] were reported, and Fe metal particles were obtained by using NaOH [7]. Smaller Fe metal particles are easily oxidized to produce iron oxide particles. Iron carbide particles have yet to be produced by the polyol method.

2 Experimental

The procedure used to produce iron oxide and iron carbide particles employed in this study resembled that described in our previous paper [4, 5]. A mixture of ferrocene (2 mmol) and 1,2-hexadecanediol (8 mmol) was dissolved in 30 mL of solvents consisting of various ratios of oleylamine (OA) and 1-octadecene (OD) in a three-necked flask equipped with a magnetic stirrer. The solution was stirred for 1 h at room temperature, and then refluxed at 300 °C for 2 h under Ar flow. After cooling to room temperature, the particles were washed by ethanol and hexane for three times, centrifuged, and dried in Ar flow. Here, we present data for five particle samples, *viz.*, P1, P2, P3, P4, and P5, which were prepared with a volume ratio OA/OD = 30/0 mL, 15/15 mL, 10/20 mL, 7/23 mL, and 3/27 mL, respectively. The samples were characterized by Mössbauer spectroscopy (Wissel, MDU1200, ^{57}Co/Rh source), X-ray diffraction (XRD; Rigaku, RINT2500, Cu-Kα), and transmission electron microscopy (TEM; Hitachi, H-9500, 300 kV).

3 Results and discussion

The shape and size of the particles were determined by TEM (Fig. 1). The particles produced in OA without OD (P1) were spherical, with 16-nm diameters. The particles produced in a

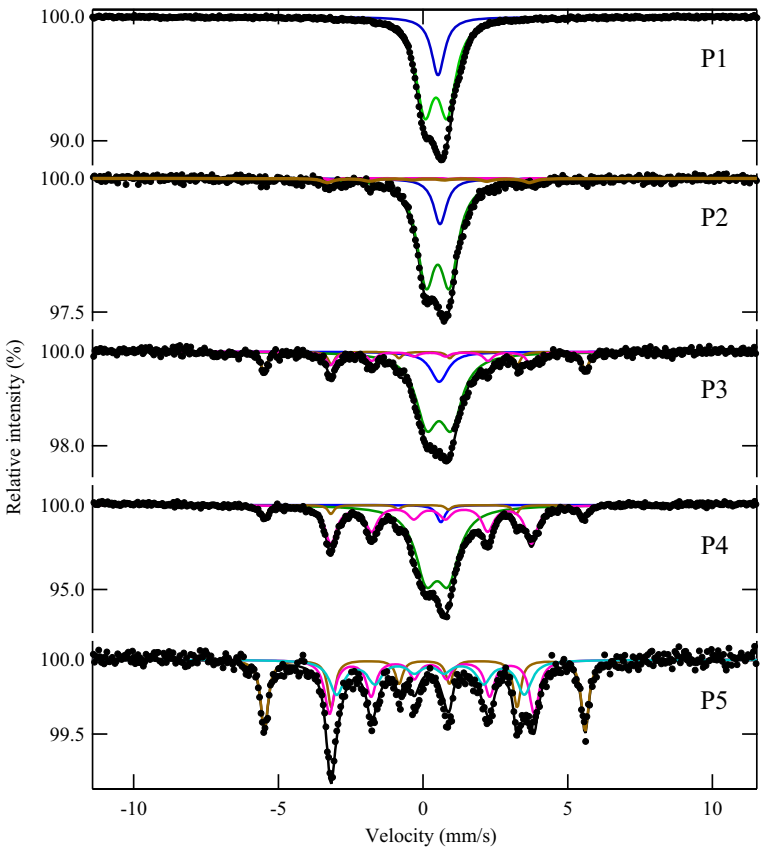

Fig. 2 Mössbauer spectra of particles measured at 293 K

mixture of OA/OD = 10/20 mL (P3) had 12-nm diameters, while those produced with the highest concentration of OD (P5, OA/OD = 3/27 mL) were the mixture of particles with various sizes. The TEM image of the particles P5 in Fig. 1 had distributed sizes ranging from 5 to 20 nm, and even larger particles with up to 150 nm diameter were observed in some other TEM images of P5. OA generally acts as a surfactant or capping reagent to protect the surfaces and thus hinders aggregation, and non-uniform sized particles were obtained with decreasing OA concentration.

Mössbauer spectra of the particles were measured at 293 K (Fig. 2); their Mössbauer parameters are tabulated in Table 1. The Mössbauer spectrum of P1 was fitted using a combination of a singlet and a doublet, both assigned to Fe^{3+} species on the basis of their isomer shifts δ. These peaks were attributed to iron oxide particles with superparamagnetic behavior; the doublet might be due to the asymmetry in the environments of Fe atoms caused by defects or particle surfaces. The spectrum of P2 had a similar shape as that of P1, and it contained a very small number of magnetic sextet components. Increasing the OD concentration (P3 and P4), the area intensities of magnetic sextets increased. The sextets were assigned to α-Fe and Fe_3C on the basis of their Mössbauer parameters. Increasing the OD concentration enhanced the Fe_3C yield. Sample P5, which was obtained at the lowest OA concentration, did not contain iron oxide; only α-Fe and Fe_3C were obtained.

Table 1 Mössbauer parameters for particles measured at 293 K

Sample	Solvent OA/OD	Component	δ mm/s	$\triangle$Eq mm/s	H T	Γ mm/s	Area int %
P1	30 mL/ 0 mL	Fe^{3+} (Singlet)	0.513(3)			0.55(1)	20.4
		Fe^{3+} (Doublet)	0.443(3)	0.78(1)		0.72(1)	79.6
P2	15 mL/ 15 mL	Fe^{3+} (Singlet)	0.50(1)			0.49(8)	14.3
		Fe^{3+} (Doublet)	0.43(1)	0.77(2)		0.72(1)	79.8
		α-Fe	−0.04(7)	0.05(14)	33.0(4)	0.29(17)	1.6
P3	10 mL/ 20 mL	Fe_3C	0.24(3)	0.04(6)	21.1(2)	0.29(8)	4.3
		Fe^{3+} (Singlet)	0.48(1)			0.70(55)	12.1
		Fe^{3+} (Doublet)	0.47(5)	0.81(10)		0.87(5)	64.9
		α-Fe	−0.01(1)	0.01(2)	33.1(1)	0.26(2)	11.7
		Fe_3C	0.19(1)	0.03(3)	20.6(1)	0.36(4)	11.3
P4	7 mL/ 23 mL	Fe^{3+} (Singlet)	0.54(2)			0.33(7)	2.8
		Fe^{3+} (Doublet)	0.41(1)	0.73(2)		0.87(2)	55.0
		α-Fe	−0.03(1)	0.02(2)	32.9(1)	0.24(2)	6.4
		Fe_3C	0.186(4)	0.05(1)	20.6(1)	0.48(1)	35.8
P5	3 mL/ 27 mL	α -Fe	−0.01(1)	0.02(1)	33.0(0)	0.29(1)	34.3
		Fe_3C (A)	0.21(1)	0.05(2)	21.1(1)	0.39(5)	34.3
		Fe_3C (B)	0.17(2)	0.04(3)	19.3(3)	0.57(5)	31.4

In order to confirm these assignments, the same samples were measured at 6 K (Fig. 3); their parameters are shown in Table 2. The Mössbauer spectrum of P1 at 6 K showed a sextet, which was assigned to γ-Fe_2O_3. The width of the sextet was broad because of the defects in the γ-Fe_2O_3 solid; the spectrum was fitted using a sextet and a component with a distributed hyperfine magnetic field (DHMF). Clearly, the superparamagnetic behavior of nanosized γ-Fe_2O_3 particles showed a singlet and doublet at 292 K. The components of the DHMF at 6 K (36.2 %) and the doublet at 293 K (20.4 %) were both attributed to the results of defects or particle surfaces, where almost half the DHMF measured at 6 K became a doublet at 293 K. The Mössbauer spectrum of P2 consisted of absorptions due to γ-Fe_2O_3, α-Fe, and Fe_3C. The DHMF component was associated with γ-Fe_2O_3 with defects. Though the Fe_3C spectrum should be a combination of two sextets as it has two Fe sites, the Fe_3C yield was too small to fit using two sextets in this sample. Therefore, Fe_3C was fitted using one sextet. In the P3 spectrum, the areas of peaks due to α-Fe and Fe_3C became large, and the DHMF distribution shifted to smaller hyperfine magnetic fields. The P4 spectrum had larger peak areas for Fe_3C, and the distribution of DHMF became small as a result of the large density of defects. The P5 particles produced at the highest OD concentration (OA/OD = 3/27 mL) did not have a γ-Fe_2O_3 component; only α-Fe and Fe_3C were observed.

The XRD patterns for the samples (Fig. 4) were in agreement with the Mössbauer spectroscopy results. The assignments of the diffraction pattern were made according to a database [8]. The P1 particles produced in OA without OD were confirmed to be γ-Fe_2O_3; the XRD pattern showed broad peaks because of the large density of defects, and some small peaks at $2\theta = 28.7°, 32.06°, 57.64°$ remained unassigned. With the addition of OD (P2, P3, and P4), the intensities of peaks associated with α-Fe and Fe_3C increased. The XRD pattern for P5 showed peaks due to α-Fe and Fe_3C, but not γ-Fe_2O_3. The average size of the γ-Fe_2O_3 nanocrystallites was estimated using the Debye-Scherrer approximation. From the

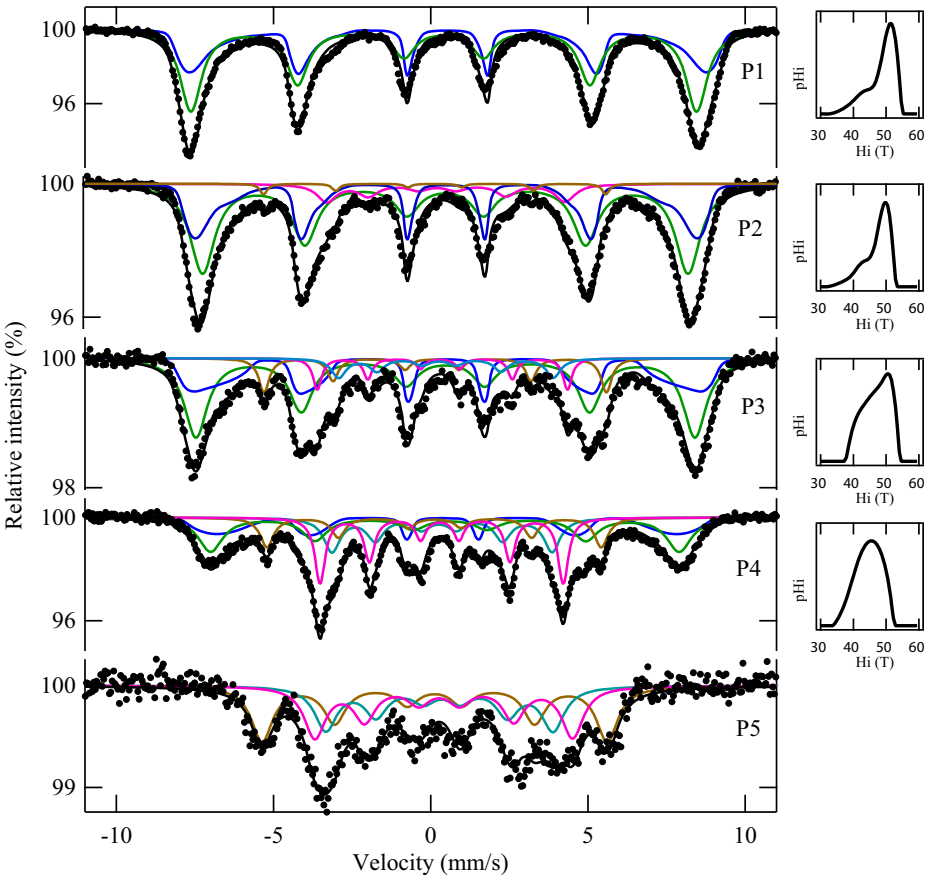

Fig. 3 Mössbauer spectra of particles measured at 6 K. The distributions of hyperfine magnetic fields corresponding to these spectra are indicated on the right-hand side

(hkl) = (440) peaks, the average sizes were calculated to be 7.4, 6.9, 6.2, and 7.6 nm for P1, P2, P3, and P4, respectively, assuming a spherical particle shape. The average diameter of γ-Fe_2O_3 nanocrystallites was estimated to be 7.0 nm, while the TEM images showed that the particle sizes were 12-16 nm.

Generally, it is hard to estimate the actual size of γ-Fe_2O_3 particles from the shapes of superparamagnetic peaks in Mössbauer spectra. Room-temperature (RT) Mössbauer spectra of γ-Fe_2O_3 particles with various sizes (10-60 nm) have been reported in the literature [9]; some magnetic sextets as well as superparamagnetic components were observed even for 10- to 20-nm γ-Fe_2O_3 particles. As the Mössbauer spectra of γ-Fe_2O_3 particles in our experiment did not show magnetic sextets at RT, the particles were smaller than 10 nm. Another study reported Mössbauer spectra of γ-Fe_2O_3 nanoparticles (5.7 nm) at RT, 77 K, and 4.2 K [10], which agreed with the Mössbauer spectra in our study, showing magnetic sextets only at low temperatures. Taking into account those results, the size of γ-Fe_2O_3 particles in our study was estimated to be smaller than 10 nm, which is also in agreement with the results calculated based on the peak widths in the XRD patterns. The larger particles

Table 2 Mössbauer parameters for particles measured at 6 K

Sample	Component	δ mm/s	$\triangle$Eq mm/s	H T	Γ mm/s	Area int %
P1	DHMF	0.54(1)	0.02(1)	52*		36.3
	γ-Fe_2O_3	0.41(1)	0.00(1)	49.8(1)	0.82(2)	63.7
P2	DHMF	0.49(1)	0.01(1)	50*		33.3
	γ-Fe_2O_3	0.46(1)	−0.05(1)	47.8(1)	0.86(2)	55.7
	α-Fe	0.12(3)	0.07(5)	33.6(2)	0.28(8)	2.0
	Fe_3C	0.34(3)	0.27(6)	23.5(2)	0.75(6)	9.0
P3	DHMF	0.50(1)	0.02(3)	50*		29.0
	γ-Fe_2O_3	0.46(1)	−0.06(1)	49.1(1)	0.89(3)	46.8
	α-Fe	0.09(1)	0.10(3)	33.7(1)	0.41(4)	9.6
	Fe_3C (A)	0.33(1)	0.07(2)	24.6(1)	0.33(5)	7.3
	Fe_3C (B)	0.37(3)	0.22(5)	21.2(3)	0.55(9)	7.3
P4	DHMF	0.44(2)	0.13(5)	46*		18.0
	γ-Fe_2O_3	0.53(2)	−0.17(4)	46.2(1)	0.94(2)	27.1
	α-Fe	0.12(1)	−0.03(2)	32.9(1)	0.52(4)	13.4
	Fe_3C (A)	0.313(5)	0.06(1)	24.0(1)	0.40(3)	22.9
	Fe_3C (B)	0.31(1)	0.10(3)	21.7(2)	0.63(4)	18.5
P5	α-Fe	0.08(2)	0.00(4)	34.1(1)	0.83(4)	36.4
	Fe_3C (A)	0.33(2)	0.15(4)	25.4(1)	0.82(10)	33.6
	Fe_3C (B)	0.31(2)	−0.06(5)	22.6(2)	0.86(8)	30.0

* Hyperfine magnetic field at the mode of the distribution

(12-16 nm) observed in TEM images might be assigned to aggregates of smaller γ-Fe_2O_3 crystallites, rather than single crystals.

As shown above, the production of γ-Fe_2O_3 was enhanced by OA, and OD acted as a carbon source to produce Fe_3C. Though the reaction mechanism in the polyol process is not well understood, it is clear that polyol reduces Fe^{2+} or Fe^{3+} cations into Fe^0 [7]. The reactions in the present study might be similar to those suggested in the literature [11], i.e., the decomposition of ferrocene $Fe(C_5H_5)$ in 1,2-hexadecanediol producing Fe^0:

$$RCHOHCH_2OH \rightarrow RCH_2CHO + H_2O \quad (1)$$

$$2RCH_2CHO + Fe(C_5H_5)_2 \rightarrow RCH_2COCOCH_2R + 2C_5H_6 + Fe^0 \quad (2)$$

where $R = CH_3(CH_2)_{13}$

In general, OA was used as both a solvent and a capping reagent for nanocrystals, whereas OD was used as a non-coordinating solvent. Many studies have reported the production of iron oxides using OA without adding polyol: iron oxide (Fe_3O_4) particles were produced by the decomposition of $Fe(acac)_3$ in benzyl ether and OA [12], and monocrystalline γ-Fe_2O_3 tetrapods were synthesized from $Fe(CO)_5$ in solution with OA [13]. In those methods, OA was employed as a surfactant or stabilizer to protect the surface of nanoparticles, but Fe^0 was not stabilized and iron oxides were eventually obtained. The growth kinetics have been studied using CdSe nanocrystals, and the role of capping agents was investigated [14]. Two processes, nucleation and particle growth, are important in the

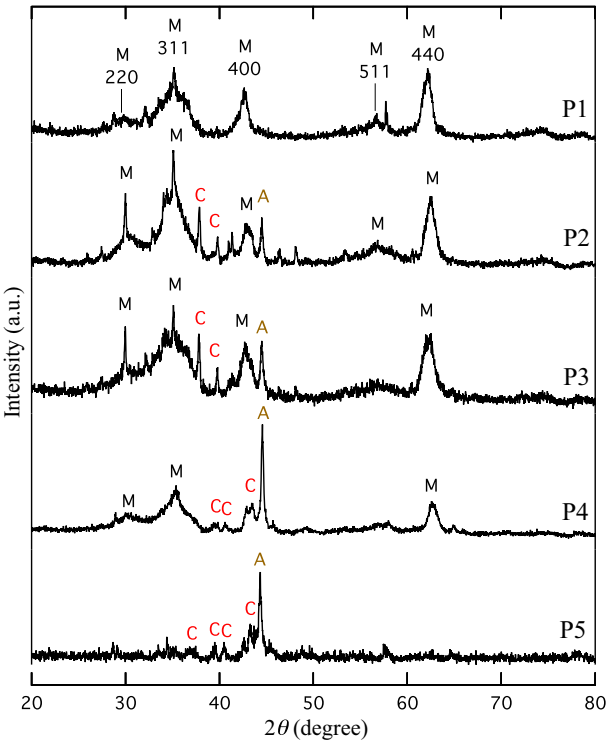

Fig. 4 XRD patterns for the particles. The labels M, C, and A correspond to γ-Fe_2O_3, Fe_3C, and α-Fe, respectively

process of particle formation. The capping reagent OA hinders agglomeration, and at the same time, it coordinates with monomers and precursors, suppressing nucleation. Therefore, the presence of an excess amount of OA reduces the nucleation rate and leads to smaller nuclei, and then it leads to larger particle sizes during the aggregation process. Similar effects were observed in our system: an excess of OA produced larger particles, but small Fe^0 precursors were oxidized, reacting with H_2O to form iron hydrates during aggregation. Then, it resulted in the production of iron oxide particles.

In contrast, OD is a non-coordinating solvent that acts as a carbon source for iron carbide precursors, and also prevents oxidation of the α-Fe particles. The Mössbauer spectrum of P5 at RT (Fig. 2) consisting of α-Fe and Fe_3C did not show superparamagnetism. A critical particle size for superparamagnetism in α-Fe and Fe_3C at RT is not well defined, as it is complicated by contribution of particle shape and surrounding materials. When the particle size is below about 10-20 nm, the particles become superparamagnetic at RT [15]. The XRD peak of α-Fe in P5 (Fig. 4) was relatively sharp; the average size was calculated to be 27 nm using the Debye-Scherrer approximation. The XRD peaks of Fe_3C were too weak to estimate the size. The Mössbauer spectrum at RT and XRD peak width indicated that the main components of P5 were the particles with larger diameter, though a lot of smaller particles less than 10 nm were observed in the TEM image of P5. To the best of our knowledge, these are the first results demonstrating the production of Fe_3C particles using a polyol method.

4 Conclusions

Iron oxide, iron carbide, and α-Fe particles were successively produced by a polyol method. The decomposition of ferrocene in 1,2-hexadecanediol produced Fe^0 precursors. The OA/OD ratio was varied to determine the effect on the particle composition. At high OA concentrations, γ-Fe_2O_3 particles with 12-16 nm diameters were obtained. At low OA concentrations, particles consisting of Fe_3C and α-Fe with various sizes were obtained. OA acted as a capping reagent, hindering nucleation and leading to a uniform particle size. At low OA concentrations, OD acted as a carbon source, Fe_3C nuclei formed as a precursor, and Fe_3C particles with various sizes were obtained.

References

1. Schnepp, Z., Wimbush, S.C., Antonietti, M., Giordano, C.: Chem. Mater. **22**, 5340 (2010)
2. Sun, S., Zeng, H., Robinson, D.B., Raoux, S., Rice, P.M., Wang, S.X., Li, G.: J. Am. Chem. Soc. **126**, 273 (2004)
3. Redl, F.X., Cho, K.S., Murray, C.B., O'Brien, S.: Nature **423**, 968 (2003)
4. Shimizu, R., Kubono, I., Kobayashi, Y., Yamada, Y.: Hyperfine Interact. **231**, 115 (2015)
5. Shimizu, R., Yamada, Y., Kobayashi, Y.: J. Radioanal. Nucl. Chem. **303**, 1473 (2015)
6. Sun, S., Murray, C.B., Weller, D., Folks, L., Moser, A.: Science **17**, 1989 (2000)
7. Joseyphus, R.J., Kodama, D., Matsumoto, T., Sato, Y., Jeyadevan, B., Tohji, K.: J. Magn. Magn. Mater. **310**, 2393 (2007)
8. JCPDS 25-1402, JCPDS 03-0989, JCPDS 87-0721
9. Siddique, M., Ahmed, A., Butt, N.M.: Phys. B **405**, 3964 (2010)
10. Guivar, J.A.R., Bustamante, A., Flores, J., Santillan, M.M., Osorio, A.M., Martinez, A.I., Valladares, L.D.L.S., Barnes, C.H.W.: Hyperfine Interact. **224**, 89 (2014)
11. Cheng, C., Xu, F., Gu, H.: New J. Chem. **35**, 1072 (2011)
12. Xu, Z., Shen, C., Hou, Y., Gao, H., Sun, S.: Chem. Mater. **21**, 1778 (2009)
13. Cozzoli, P.D., Snoeck, E., Garcia, M.A., Giannini, C., Guagliardi, A., Cervellino, A., Gozzo, F., Hernando, A., Achterhold, K., Ciobanu, N., Parak, F.G., Cingolani, R., Manna, L.: Nano Lett. **6**, 1966 (2006)
14. Bullen, C.R., Mulvaney, P.: Nano Lett. **4**, 2303 (2004)
15. Amulyavichus, A.P., Suzdalev, I.P.: Sov. Phys. JETP. **37**, 857 (1973)